



Electronic phase diagram in the half-filled ionic Hubbard model with site-dependent interactions

Anh-Tuan Hoang^{a,*}, Thi-Hai-Yen Nguyen^a, Duc-Anh Le^b

^a Institute of Physics, Vietnam Academy of Science and Technology, Viet Nam

^b Faculty of Physics, Hanoi National University of Education, Xuan Thuy 136, Cau Giay, Hanoi 10000, Viet Nam

ARTICLE INFO

Keywords:

Metal-insulator transitions
Ionic Hubbard model
Site-dependent interactions
Coherent potential approximation

ABSTRACT

The ionic Hubbard model with spatially alternating interactions, which may be realized by cold atoms in optical lattices, is studied by mean of the coherent potential approximation. The paramagnetic phase diagram for the half-filled model at zero temperature is obtained. The possibility of enlarging an intermediate metallic region in the parameter space is addressed.

1. Introduction

The ionic Hubbard model (IHM) with alternating site energies was originally proposed to study the neutral-ionic in organic charge-transfer salts [1]. Later this model have been used for describing various phenomena in correlated electron systems such as the enhanced response of quasi-one-dimensional ferroelectric perovskites [2], the evolution of electronic structure in $\text{SrRu}_{1-x}\text{Ti}_x\text{O}_3$ [3], and unconventional spin-singlet superconductivity in layered nitrides $\beta\text{-MnCl}$ [4]. It has been established that at half-filling the on-site Coulomb interaction can lead electrons to a localization which yields a Mott insulating state; while the ionic potential that takes alternating values on neighboring sites of a bipartite lattice (sublattices A and B) results in a band insulating phase. Up to now, in most studies, the on-site Coulomb interaction was supposed to be the same for both types of sites ($U_A = U_B$). However, that is hardly to justify in real situation. In $\text{SrRu}_{1-x}\text{Ti}_x\text{O}_3$, for example, Ti is a 3d-metal and Ru is a 4d-metal, consequently we have different local electronic interactions for Ti and Ru sites. Therefore, the IHM with site-dependent interactions can be regarded as more realistic ionic model for describing the above phenomena in correlated electron systems.

Another motivation for our investigation of the IHM with alternating interactions originates from the fact that many of theoretical studies have revealed the emergence of an intermediate phase between the band insulator (BI) and the Mott insulator (MI). In one dimension it was found by the bonization method that a spontaneously dimerized insulating shows up between the BI and the MI [5,6], which was confirmed subsequently in the density matrix renormalization group studies [7,8]. As to the nature of the intermediate phase in two and higher

dimensions, there is some controversy: the cellular dynamical mean field theory (DMFT) [9] or the variational cluster approach [10] predicted a bond ordered phase, while a metallic phase was obtained by the determinant quantum Monte Carlo method [11], the single site DMFT [12–14] or the coherent potential approximation (CPA) [15]. Here it is remarkable that in both cases the intermediate phase only occupies a narrow region in the phase diagram, which cast additional on the investigation of its properties. By using the IHM with alternating interactions we can explore the possibility of enlarging the intermediate region in the parameter space by varying the ratio U_B/U_A .

It should be noted that with the achievement of laser cooling technique the physics of the IHM may find a realization in optical lattices which can be generated in various geometries, including bipartite lattice with different interactions and potential minima on the sublattices [16,17]. It provides a cleaner and tunable platform compared with real materials for probing open questions in the physics of strongly correlated system.

The purpose of this paper is to study the electronic phase diagram in the half-filled IHM with site-dependent interactions by mean of the coherent potential approximation. This method is well suited to study the metal-insulator transitions in the conventional IHM [15]. Assuming a paramagnetic solution, we focus on the effect which appears due to $U_A \neq U_B$.

2. Model and solving method

We consider the following IHM with alternating interactions in dimensions $D \geq 2$ on a bipartite lattice (sublattices A and B)

* Corresponding author.

E-mail address: hatuan@iop.vast.ac.vn (A.-T. Hoang).

$$H = -t \sum_{\langle ij \rangle \sigma} (c_{i\sigma}^\dagger c_{j\sigma} + \text{H.c.}) + \varepsilon_A \sum_{i \in A} n_i + \varepsilon_B \sum_{i \in B} n_i + \sum_{\alpha, i \in \alpha} U_\alpha n_{i\uparrow} n_{i\downarrow}, \quad (1)$$

where $c_{i\sigma}$ ($c_{i\sigma}^\dagger$) annihilates (creates) an electron with spin σ at site i , $n_{i\sigma} = c_{i\sigma}^\dagger c_{i\sigma}$, $n_i = n_{i\uparrow} + n_{i\downarrow}$ and the sum $\langle ij \rangle$ is the sum over nearest neighbor sites of the lattice. U_α is the site-dependent Coulomb repulsion in the sublattice α ($\alpha = A, B$), $\varepsilon_A = \Delta$, $\varepsilon_B = 0$ the ionic energies, and the energy difference between the two types of sites Δ is chosen as a positive value. The same model in dimension $D = 1$, as far as we know, were first employed to study effects of strong electron correlation on the electron-lattice interaction [2].

In the alloy-analog approach the many-body Hamiltonian is replaced by a one-particle Hamiltonian of the form

$$\tilde{H} = \sum_{i \in A\sigma} E_{A\sigma} n_{i\sigma} + \sum_{i \in B\sigma} E_{B\sigma} n_{i\sigma} - t \sum_{\langle ij \rangle \sigma} (c_{i\sigma}^\dagger c_{j\sigma} + \text{H.c.}), \quad (2)$$

where the random potential $E_{\alpha\sigma}$ takes the values $\varepsilon_\alpha^{(v)}$ ($v = \overline{1, 2}$) with the probabilities $p_{\alpha\sigma}^{(v)}$

$$E_{\alpha\sigma} = \begin{cases} \varepsilon_\alpha = \varepsilon_\alpha^{(1)}, & p_{\alpha\sigma}^{(1)} = 1 - n_{\alpha-\sigma}, \\ \varepsilon_\alpha + U_\alpha = \varepsilon_\alpha^{(2)}, & p_{\alpha\sigma}^{(2)} = n_{\alpha-\sigma}. \end{cases} \quad (3)$$

The mean occupation numbers $n_{A-\sigma}$ and $n_{B-\sigma}$ must be determined self-consistently. We focus on the paramagnetic case, for which $n_{A\sigma} = n_{A-\sigma} = n_A/2$, $n_{B\sigma} = n_{B-\sigma} = n_B/2$ and all the one-electron quantities become spin-independent. The structure of a bipartite lattice leads to a local Green function of the form

$$G_\alpha(\omega) = (\omega - \Sigma_\alpha) \int \frac{\rho_0(E) dE}{(\omega - \Sigma_A)(\omega - \Sigma_B) - E^2}, \quad (4)$$

where $\alpha = A(B)$ and $\bar{\alpha} = B(A)$, Σ_α is the self-energy for α -sublattice, $\rho_0(E)$ is the density of states (DOS) for non-interacting electrons. By employing Hubbard's semi-elliptic DOS $\rho_0(E) = \frac{2}{\pi W^2} \sqrt{W^2 - E^2}$ with W being the half-width of the band, the local Green function is then given by [18]

$$G_\alpha(\omega) = \frac{2}{W^2} \left\{ \omega - \Sigma_\alpha - \left[(\omega - \Sigma_\alpha)^2 - \frac{\omega - \Sigma_\alpha}{\omega - \Sigma_\alpha} W^2 \right]^{1/2} \right\}. \quad (5)$$

The CPA demands that the scattering matrix vanishes on average over all possible disorder configurations. This is equivalent to

$$G_\alpha(\omega) = \sum_{v=1}^2 p_\alpha^{(v)} G_\alpha^{(v)}(\omega), \quad (6)$$

where

$$G_\alpha^{(v)}(\omega) = \frac{G_\alpha(\omega)}{1 - (\varepsilon_\alpha^{(v)} - \Sigma_\alpha(\omega)) G_\alpha(\omega)}. \quad (7)$$

The equations (5)–(7) must now be solved with $n_A + n_B = 2$, where at zero temperature $n_\alpha = -2/\pi \int_{-\infty}^{E_F} \Im G_\alpha(\omega) d\omega$ with E_F the Fermi energy. From the self-consistent CPA solution one can determine the local one-particle DOS $\rho_{A/B}(\omega)$, the occupation numbers n_A, n_B and the double occupancy d_A, d_B as functions of the model parameters Δ, U_A and U_B . A metal is distinguished from an insulator by a finite total DOS at the Fermi level $\rho(E_F) = \rho_A(E_F) + \rho_B(E_F)$.

3. Results and discussion

Before numerical solving the equations (5)–(7), let us briefly consider limiting case. In the model with uniform interaction, setting $U_A = U_B = U$ and shifting the one-electron energy by $-U/2$, we reproduce the CPA equation for the Green function in the conventional IHM [15] in which the metallic phase of the system can be found between BI and MI phases. In addition, the metallic region is sandwiched between $U_{c1}(\Delta)$ and $U_{c2}(\Delta)$, where $\Delta < U_{c1}(\Delta) < U_{c2}(\Delta) < \sqrt{\Delta^2 + W^2}$, keeping in

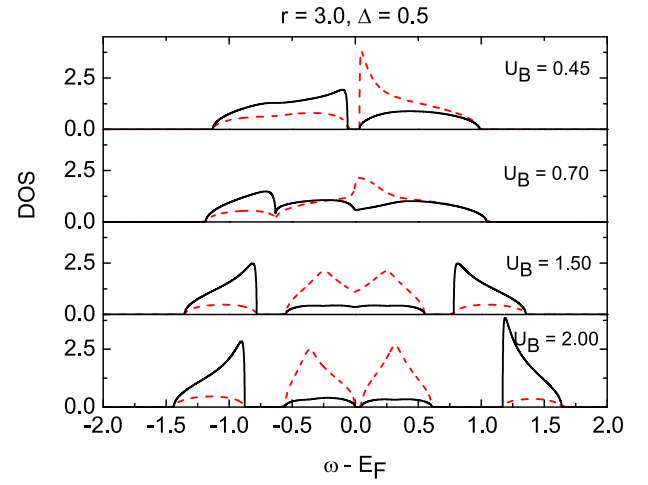


Fig. 1. Local DOS for the A-sublattice (dashed lines) and for the B-sublattice (solid lines) for various values of U_B , for $r = 3.0$ and $\Delta = 0.5$. Energy $\omega - E_F$ and parameters Δ, U_B are in energy unit set by $W = 1$.

mind that in the present paper the energy difference between the two types of sites is Δ .

We turn now to present our numerical results. Through this work we set W as the unit of the energy and denote $r = U_B/U_A$. Fig. 1 shows the local DOS for each type of sites $\rho_A(\omega)$ and $\rho_B(\omega)$ for $r = 3, \Delta = 0.5$ and four values of U_B . The general appearance of the DOS displays four structures. Two of these structures are mainly composed of A-states (dashed lines) and the other two of B-states (solid lines). The two structures of α -states can be interpreted as a lower Hubbard (LHB) and an upper Hubbard band (UHB) separated by U_α . For $U_B = 0.45$ and 2.0 , corresponding to the band insulating and Mott insulating phases, the DOS show a gap around the Fermi level E_F . In contrast, the DOS at E_F for $U_B = 0.70$ and 1.50 are nonzero, which indicate a metallic phase. For comparison, the results for the same parameters for the conventional IHM ($r = 1.0$) are plotted in Fig. 2. The curves for $U_B = 0.45, 0.70$ are similar to that of $r = 3$, indicating that for relatively small values of U_B the effect of alternating interactions is small. On the other hand, for $U_B = 1.50$ two of A-states are separated at $r = 1.0$ ($U_A = 1.5$) while its splitting does not occur at $r = 3.0$ ($U_A = 0.5$), the total DOS has four structures and the Fermi level lays in the gap, so the system becomes the insulator. For $U_B = 2.0$ the system is the MI with the gap, which is much larger than the those of $r = 3.0$.

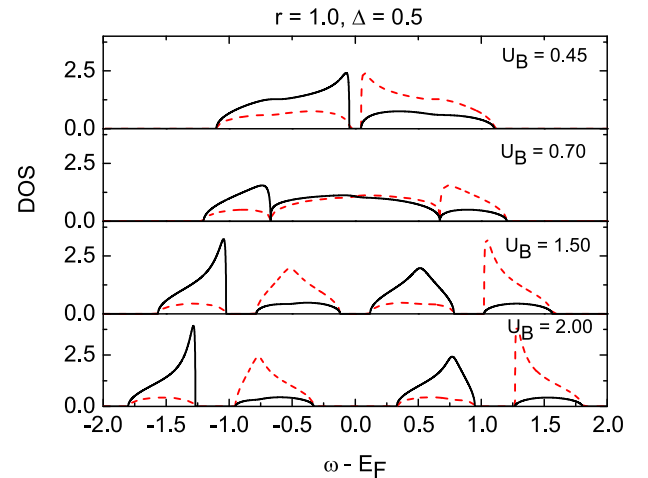


Fig. 2. Local DOS for the A-sublattice (dashed lines) and for the B-sublattice (solid lines) for the same values of U_B as in Fig. 1, for $r = 1.0$ and $\Delta = 0.5$.

The phase diagram $\Delta - U_B$ at zero temperature for the system for $r = 0.5, 1.0, 2.0$ and 3.0 is shown in Fig. 3. It can be seen that the phase boundary between the BI and metallic phases is almost independent on r and approaches the line $U_B = \Delta$. This result can be understood as follows: Because Δ was chosen to be positive, the upper Hubbard band of A is always nearly empty. Consequently, when Δ is fixed and local interaction U_B is switched on and gradually increased, the hopping of electrons from the upper Hubbard band of B to the lower Hubbard band of A occurs when these bands begin to overlap, i. e. when U_B approaches to Δ . Therefore, the system undergoes a transition from the BI to the metallic state for $U_B \approx \Delta$, independent on U_A , i. e. on r . On the other hand, the phase boundary for the metal and MI is significantly dependent on r in weak-coupling regime, but again approaches the strong coupling line $U_B = \Delta$ as Δ is increased. This is due to the effect of splitting band of A-states. For small U_A (larger r) two structures of A-states are not separated (Compare Figs. 1 and 2, for the same $U_B = 1.50$), therefore the transition from metal to Mott insulator is significantly delayed resulting in a larger critical value for U_B . It is interesting to note that the enlargement of the metallic regime has also been found in the conventional IHM by using CPA with including intersite spatial correlations [19] as well as in the bilayer IHM [20]. We note that for $\Delta = 0$ this behavior is agreement with the results of both Saitou *et al.* [21] and Le *et al.* [22] for the Hubbard model with site-dependent interactions, where according to their studies the critical interactions for the metal to MI transition are given by $U_A U_B = \text{const}$, hence the critical value for U_B increases with increasing r .

To clarify the nature of phase transitions and the insulating states we calculate the staggered charge density $n_B - n_A$ and double occupancy $d_\alpha = \langle n_{\alpha\uparrow} n_{\alpha\downarrow} \rangle$ with α being A and B. These quantities are plotted in Figs. 4 and 5 for $r = 3.0$, $\Delta = 0.5$ and 2.0 . For small U_B , only B sites are occupied and A sites are almost empty, correlation effects are weak in the occupied B band, so $n_B - n_A$ and d_B are large, d_A is small. The corresponding insulating state is clearly a band insulator. As U_B is increased, the double occupancy rapidly decreases for B sites. For larger U_B , both types of site are strongly correlated with almost zero double occupancy and the charge density approaches zero. Therefore, the insulating state is a Mott insulator. Like the conventional IHM, in the IHM with site-dependent interactions, the density charge curves change in slopes just after $U_B = \Delta$ for both values of Δ . As noted in Ref. [19], these indicate the BI to the metal transition which is dominated by the charge density wave. On the other hand, the MIT is governed by the Hubbard U_α

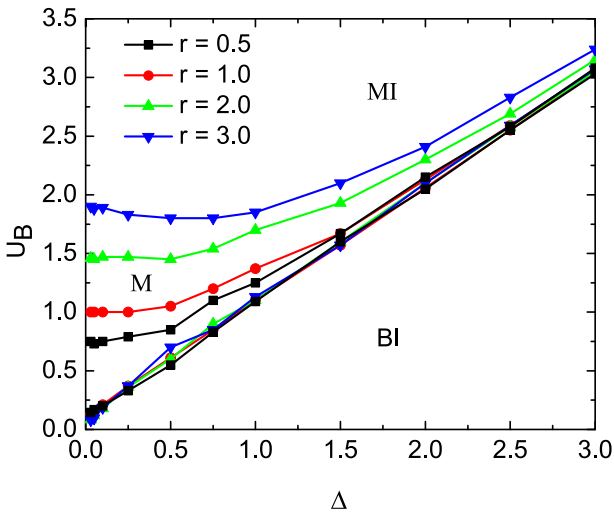


Fig. 3. $T = 0$ phase diagram of the IHM with site-dependent interactions for different values of r . MI, M and BI denote Mott insulator, metal and band insulator, respectively. The phase boundary between BI and metal is almost independent on r and approaches the line $U_B = \Delta$ for $\Delta > 0.5$, whereas the phase boundary between metal and MI is significantly dependent on r in weak-coupling regime.

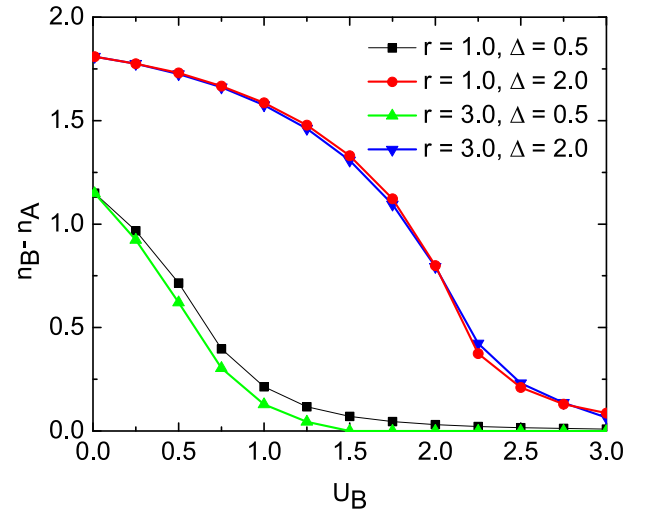


Fig. 4. Staggered charge density $n_B - n_A$ as a function of U_B for $\Delta = 0.5$ and 2.0 . Like the conventional IHM, in the IHM with $r = 3.0$, the density charge curves change in slopes just after $U_B = \Delta$ for both values of Δ . In CPA the phase transitions are clearly continuous.

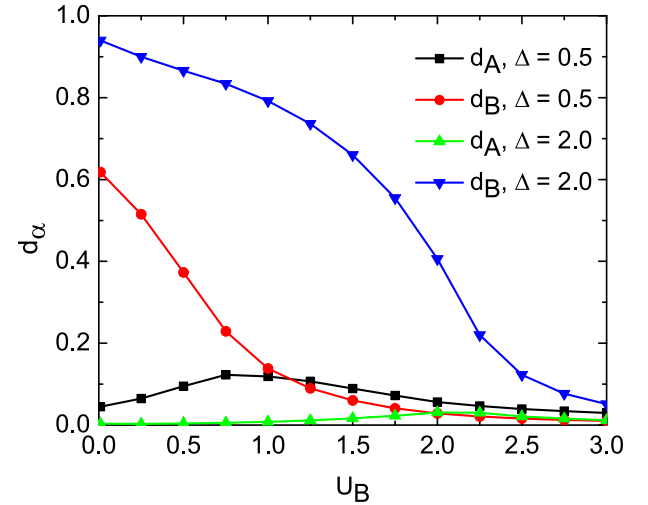


Fig. 5. Double occupancies d_A and d_B in the IHM with $r = 3.0$ as a function of U_B for $\Delta = 0.5$ and 2.0 .

and so the curves smoothly change with no inflection point at the MIT. As in the conventional IHM, the phase transitions in the IHM with site dependent interactions at zero temperature are clearly continuous.

4. Conclusions

We have studied the paramagnetic phase diagram in the half-filled ionic Hubbard model with site-dependent interactions for the Bethe lattice in the limit of infinite dimensions by means of the coherent potential approximation. As noted in Ref. [23], for the Bethe lattice of connectivity $z \geq 3$ this approximation is good, at least in a qualitative sense. Therefore, is it reasonable to believe our calculation is applicable to the IHM in dimensions $D \geq 2$. We found that while the critical value U_{Bc1} for transition from BI to metal is almost independent on the ratio $r (= U_B/U_A)$, the critical value U_{Bc2} for transition from metal to MI throughout of the range Δ increases with increasing r . Therefore, in the systems with $r \gg 1$ the metallic region significantly enlarges in comparison with that of the conventional ionic Hubbard model ($r = 1$). The nature of phase transitions and the insulating states are clarified by

calculating the staggered charge density and the double occupancy.

We hope that our investigation of the IHM with site-dependent interactions provides an useful step towards understanding the metal-insulator transitions in real systems with ionic potentials. This deserves further theoretical and experimental investigations.

Acknowledgments

This research is funded by National Foundation for Science and Technology Development (NAFOSTED) under Grant No. 103.01-2017.56.

References

- [1] J. Hubbard, J.B. Torrance, *Phys. Rev. Lett.* 47 (1981) 1750.
- [2] T. Egami, S. Ishihara, M. Tachiki, *Science* 261 (1993) 1307.
- [3] B.J. Powell, J. Merino, R.H. McKenzie, *Phys. Rev. B* 80 (2009) 085113.
- [4] T. Wantanabe, S. Ishihara, *J. Phys. Soc. Jpn.* 82 (2013) 034704.
- [5] M. Fabrizio, A.O. Gogolin, A.A. Nersisyan, *Phys. Rev. Lett.* 83 (1999) 2014.
- [6] C.D. Batista, A.A. Aligia, *Phys. Rev. Lett.* 92 (2004) 246405.
- [7] Y.Z. Zhang, C.Q. Wu, H.Q. Lin, *Phys. Rev. B* 67 (2003) 205109.
- [8] S.R. Manmana, V. Meden, R.M. Noack, K. Schonhammer, *Phys. Rev. B* 70 (2004) 155115.
- [9] S.S. Kancharla, E. Dagotto, *Phys. Rev. Lett.* 98 (2007) 016402.
- [10] H.M. Chen, H. Zhao, H.Q. Lin, C.Q. Wu, *New J. Phys.* 12 (2010) 093021.
- [11] K. Bouadim, N. Paris, F.H. Feber, et al., *Phys. Rev. B* 76 (2007) 085112.
- [12] K. Byczuk, M. Sekania, W. Hofstetter, A.P. Scalettar, *Phys. Rev. B* 79 (2009) 121103 (R).
- [13] A. Garg, H.R. Krishnamurthy, M. Randeria, *Phys. Rev. Lett.* 97 (2006) 046403.
- [14] L. Craco, P. Lombardo, R. Hayn, et al., *Phys. Rev. B* 78 (2008) 075121.
- [15] A.T. Hoang, *J. Phys.: Condens. Matter* 22 (2010) 095602.
- [16] R. Yamazaki, S. Taie, S. Sugawa, Y. Takahashi, *Phys. Rev. Lett.* 105 (2010) 050405.
- [17] M. Messer, R. Desbuquois, T. Uehlinger, et al., *Phys. Rev. Lett.* 115 (2015) 115303.
- [18] A.T. Hoang, P. Thalmeier, *J. Phys.: Condens. Matter* 14 (2002) 6639.
- [19] D.A. Rowlands, Y.Z. Zhang, *J. Phys.: Condens. Matter* 26 (27) (2014) 274201.
- [20] M. Jiang, T.C.S. Schulthess, *Phys. Rev. B* 93 (2016) 165146.
- [21] T. Saitou, A. Koga, A. Yamamoto, *J. Supercond. Nov. Magn.* 26 (2013) 17.
- [22] D.A. Le, T.T.T. Tran, A.T. Hoang, *Eur. Phys. J. B* 86 (2013) 503.
- [23] R. Vlaming, D. Vollhardt, *Phys. Rev. B* 45 (1992) 4637.